Multi Low-resolution Infrared Sensor Setup for Privacy-preserving Unobtrusive Indoor Localization

Christian Kowalski[1], Kolja Blohm[1], Sebastian Weiss[1], Max Pfingsthorn[1], Pascal Gliesche[1] and Andreas Hein[2]

[1]*OFFIS, Institute for Information Technology, Oldenburg, Germany*

[2]*Carl von Ossietzky University, Oldenburg, Germany*

Keywords: Indoor Localization, Multiple Infrared Sensors, Health Monitoring, Classification.

Abstract: The number of home intensive care patients is increasing while the number of nursing staff is decreasing at the same time. To counteract this problem, it is necessary to take a closer look at safety-critical scenarios such as long-term home ventilation to provide relief. One possibility for support in this case is the exact localization of the affected person and the caregiver. A wide variety of sensors can be used to remedy this problem. Since the privacy of the patient should not be disturbed, it is important to find unobtrusive solutions. For this specific application, low-resolution infrared sensors - which are unable to invade the patient's privacy due to the low amount of sensor data information - can be used. The objective of this work is to create a basis for an inexpensive, privacy-preserving indoor localization system through the use of multiple infrared sensors, which can be for example used to support long-term home ventilated patients. The results show that such localization is possible by utilizing a support vector machine for classification. For the described scenario, a specific sensor layout was chosen to ensure the highest possible area coverage with a minimum amount of sensor installations.

1 INTRODUCTION

Due to the growing economic pressure, the number of domestic intensive care patients is increasing (Razavi et al., 2016), not least due to the aging of the world population (World Health Organization, 2015). Especially the group of long-term home ventilated patients is exposed to high risk because even a single mistake can lead to the death of the patient. Assistive technologies can help to alleviate the risk and at the same time increase safety in such a safety-critical scenario (see Fig. 1). For this particular case, different monitoring solutions can be used to improve response time or to predict critical events in advance. Cameras offer good image quality and provide the ability to cover large areas but due to privacy concerns, they have a low acceptance rate in domestic environments (Rapoport, 2012). Consequently, multiple unobtrusive sensors distributed in the apartment or house of elders represent an alternative to normal cameras. They can provide valuable information to predict or detect frequent hazards like falls (Mubashir et al., 2013) or less frequent hazards like missing caregivers during a respiratory device alarm of patients in need of long-term home mechanical ventilation (Gerka et al., 2018).

Figure 1: Staging of a long-term home ventilation scenario. The patient is localized by the wall mounted infrared sensor cluster for security purposes. Due to the low-resolution of the sensors, the patient's privacy is not invaded.

One example of such an unobtrusive sensor that preserves privacy is a thermal infrared (IR) array sensor. This sensor is able to capture the temperature of a two-dimensional field with 8 $\times$ 8 pixels, even in

Kowalski, C., Blohm, K., Weiss, S., Pfingsthorn, M., Gliesche, P. and Hein, A.
Multi Low-resolution Infrared Sensor Setup for Privacy-preserving Unobtrusive Indoor Localization.
DOI: 10.5220/0007694601830188
In *Proceedings of the 5th International Conference on Information and Communication Technologies for Ageing Well and e-Health (ICT4AWE 2019)*, pages 183-188
ISBN: 978-989-758-368-1

darkness. In this paper, we will make use of multiple cost-efficient Panasonic thermopile low-resolution IR thermal array sensors with a 60° view angle called Grid-EYE (AMG8833) (Panasonic, 2016) to perform indoor localization.

1.1 Related Work

The use of low-resolution IR array sensors for different indoor monitoring or surveillance tasks is an emerging topic. Despite the sensor's small field of view, most of the publications focus on single Grid-EYE sensor setups to detect the presence of a person in front of the sensor (Shetty et al., 2017; Beltran et al., 2013; Trofimova et al., 2017). A ceiling mounted configuration by Trofimova et al. (2017) aimed at indoor detection in noisy environments, but only the presence of a person within the sensor's field of view is determined and not the specific location. Gonzalez et al. (2013) used a wall mounted Grid-EYE to detect different activities in a pantry area. Again, the captured data was not used to provide a location of the detected objects or persons. Further on, Gerka et al. (2018) proposed a ceiling mounted setup where one Grid-EYE sensor is used to detect the number of persons to enhance the safety of artificially ventilated persons but also again, the specific location of the detected persons was not taken into account. In contrast to the aforementioned publications, Basu and Rowe (2015) proposed a method to detect the presence of a single person based on motion tracking with a ceiling mounted Grid-EYE sensor.

Another crucial field of application of the Grid-EYE sensor is fall detection. In this case, the sensor is permanently mounted to a specific location (ceiling or wall) and tries to detect falls in its field of view (Fan et al., 2017; Mubashir et al., 2013). Again, present work makes use of only one sensor at a time to infer certain information about the movement of a person, which might have a negative impact on the accuracy of these solutions.

To our knowledge, all applications either try to detect whether or not one or more persons are within the sensor's field of view or they try to detect falls or motion in general. For this reason, in this paper we propose a method to localize a single person indoors instead of merely detecting presence. To do so, we use a setup of two IR sensor clusters, each consisting of three Grid-EYE sensors. Thus, the field of view and the amount of data is increased, which might result in a better localization accuracy. Finally, we compare the localization accuracy for a different number of Grid-EYE sensors.

2 MATERIALS AND METHODS

2.1 Hardware Setup

2.1.1 Layout

For the conducted research we make use of multiple 8×8 thermopile IR array Grid-EYE sensors. The sensor measures a size of $11.6 \times 8 \times 4.3$ mm and has the advantage that - compared to pyroelectric and single element thermopile sensors - not only motion but also presence and position are detectable due to the sensor's array alignment (Panasonic, 2016). The Grid-EYE is able to sense surface temperatures ranging from -20° up to +100° Celsius, has a 60° view angle, a human detection distance of up to 7 m, a frame rate of 10 Hz and uses an inter-integrated circuit (I2C) as an external interface option (Panasonic, 2017). Using the I2C interface, it is possible to access the sensor's digital temperature reading directly, e.g. via the CircuitPython AMG88xx module provided by Adafruit (Adafruit, 2017).

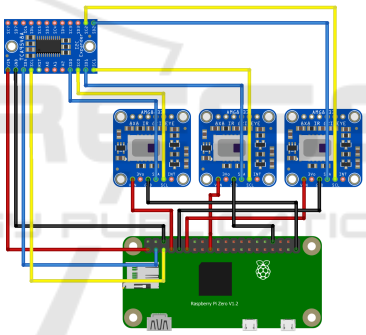

Figure 2: Circuit visualization of one Grid-EYE sensor cluster setup. One Raspberry Pi Zero is connected to three Grid-EYE sensors via a multiplexer to bypass the limited amount of only two I2C addresses.

The correct placement of the sensors plays an important role in the outcome of the experiment. While most published work prefers a ceiling mount (Trofimova et al., 2017; Beltran et al., 2013; Basu and Rowe, 2015; Mashiyama et al., 2015; Gerka et al., 2018), wall mounted configurations are also used (Fan et al., 2017; Jeong et al., 2014; Gonzalez et al., 2013; Mubashir et al., 2013). It is further stated that the wall mounted setup has several drawbacks like an obstructed view due to furniture and a varying amount of pixels representing a person based on the distance to the sensor (Trofimova et al., 2017). While the former explained disadvantage is dependent on each local room layout and can also occur when mounted on the ceiling, the latter does not really represent a disadvantage if several sensors are distributed so that the

varying pixel amount can be used as an implicit indicator for distance. Depending on the height of the ceiling, the ceiling mounted setup might only cover a small area and in most cases will not make use of the maximum person detection distance of 7 m. Overall, the positioning depends on the spatial conditions and the activity to be observed. In perspective, however, one can assume that a combination of the two positioning options is also conceivable.

2.1.2 Sensor Cluster

Three interconnected sensors are required for a desirable area coverage of 180°. This creates the problem that only two fixed I2C addresses are available, which is why a multiplexer is used in our setup in addition to the three IR sensors. Using a multiplexer, a separate switching between the sensor channels becomes possible (see Fig. 2).

In our setup, each sensor cluster is comprised of three Grid-Eye sensors, a multiplexer for the recording and a Raspberry Pi Zero for the wireless transmission of the data. Since the exact positioning plays an important role for a coverage of 180°, a special case for wall mounting was 3D-printed based on previous work. All necessary elements can be installed and fastened on the wall in the 3D-printed case for measurements (see Fig. 3).

Figure 3: The image shows a complete sensor cluster setup, ready to be mounted on the wall. A Raspberry Pi Zero, a multiplexer and three Grid-EYE sensors are installed in the 3D-printed case. The sensors are aligned in such a way that a 180° horizontal and 60° vertical field of view is achieved.

2.2 Indoor Localization Experiment

The cluster presented in the previous chapter for the acquisition of Grid-EYE IR sensor data was assembled in two copies so that a total of six sensors were available for measurements. In the course of the experiment, different layouts were compared for localization in the domestic environment. Figure 5 shows that the use of only one sensor results in many blind spots. Thus, a room can not be completely captured. However, in the case of monitoring in a domestic environment, it is important to cover the largest possible area to guarantee safety. For this reason, this paper focuses on the localization accuracy of two 180° sensor clusters attached to the walls perpendicular to each other. The difference in the measurement area covered by one or two clusters is negligible depending on the layout of the room, but the additional sensor information from a different angle may be important for the accuracy of the localization method, especially when one considers the low-resolution of the sensor (see. Fig. 4).

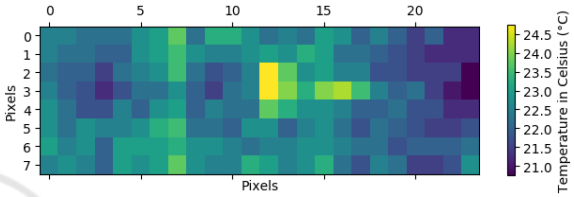

Figure 4: Exemplary Grid-EYE sensor cluster output that shows a 8 × 24 pixel temperature (C°) matrix. It is quite obvious that no identifying information can be captured with this sensor.

Since a ground truth of the position is necessary for a correct verification of the localization results, the position of the recorded person must be recorded in addition to the sensor data of the IR sensors. For this purpose, the localization sensors of the Windows Mixed Reality headset Dell Visor with inside-out tracking were used. Other tracking solutions, often based on IR illumination themselves, were not chosen to eliminate possible interference. Although the tracking precision of virtual reality headsets seems debatable in certain scientific fields (Niehorster et al., 2017), this does not hold in our case due to the extreme mismatch with the low-resolution of the Grid-EYE sensors.

The measurements of the experiment are conducted as follows: after placing the sensor clusters on the walls at a height of about 1.5 m, the person to be measured is equipped with the Dell Visor headset on a predefined measuring area of 2.5 × 1.5 m. A data logger explicitly written for this measurement captures the x- and y-coordinates of the headset while the six Grid-EYE sensors capture their respective 8 × 8 matrices of temperature (see Fig. 6), both with a frame rate of 10 Hz. The person with the headset simultaneously sees a predefined area in the virtual reality that corresponds to the measuring surface in reality in order to prevent accidental collision with objects in the room. The collected data is used for the classification to perform the indoor localization.

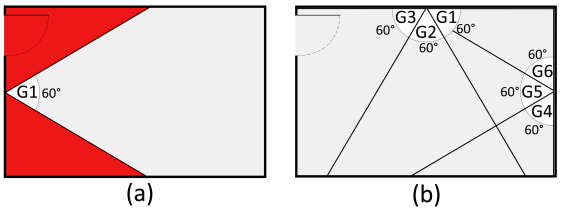

Figure 5: Top-down perspective on an exemplary room with different sensor placement layouts. Red colored areas are blind spots. (a) Only one Grid-EYE sensor (G1) misses a large area of the room during capture. (b) With two clusters (G1-G3, G4-G6) the whole room can be captured. These layouts do not provide a great advantage regarding the captured area compared to the layout with only one cluster, but they have an impact on the indoor localization accuracy.

2.3 Classification

A classification procedure is used to process the stored temperature and position data. Assuming that the recorded position data can serve as a ground truth for localization, supervised learning can be used to train a classifier. For this purpose, the measuring surface is divided into a grid of 50 × 50 cm fields, which serve as a label for the applied support vector machine (SVM) classifier. In general, a SVM tries to find a hyperplane in a n-dimensional space in order to separate classes based on the input data. On the basis of label pairs $(\boldsymbol{x}_i, y_i), i = 1, ..., l$ where $\boldsymbol{x}_i \in \mathbb{R}^n$ is the feature vector and $\boldsymbol{y} \in \{1, -1\}^l$ is the class label vector, the used C parameter SVM tries to solve the following optimization problem:

$$\min_{\boldsymbol{w},b,\zeta} \quad \frac{1}{2}\boldsymbol{w}^T w + C\sum_{i=1}^{l}\zeta_i \qquad (1)$$

$$\text{subject to} \quad y_i(\boldsymbol{w}^T\phi(\boldsymbol{x}_i) + b) \geq 1 - \zeta_i, \qquad (2)$$

$$\zeta_i \geq 0, i = 1, ..., n, \qquad (3)$$

where $C > 0$ depicts the error term's penalty parameter, $\boldsymbol{w}$ is the coefficient vector, b is a constant, ζ_i is a parameter vector and the training vectors $\boldsymbol{x}_i$ are mapped into a higher, maybe even infinite dimensional space through function ϕ (Hsu et al., 2003). The kernel function used in our particular case is a third degree polynomial with a parameter $C = 1$. No hyper-parameter tuning was performed in this case. For the implementation, an already existing machine learning library in Python is used (Pedregosa et al., 2011). The following accuracy function was used to determine the correct predictions over $l_{samples}$, where $\hat{y}_i$ is the predicted value of the i-th sample and y_i is the corresponding true value:

$$\text{accuracy}(y, \hat{y}) = \frac{1}{l_{samples}} \sum_{i}^{l_{samples}-1} 1(\hat{y}_i = y_i). \qquad (4)$$

The feature vector consists of all corresponding temperature values of the Grid-EYE sensors and the labels correspond to each predefined 50 × 50 cm grid field, which can also be seen in Fig. 6. In addition, we will compute the accuracy for a correct classification within a neighborhood of four for comparison purposes.

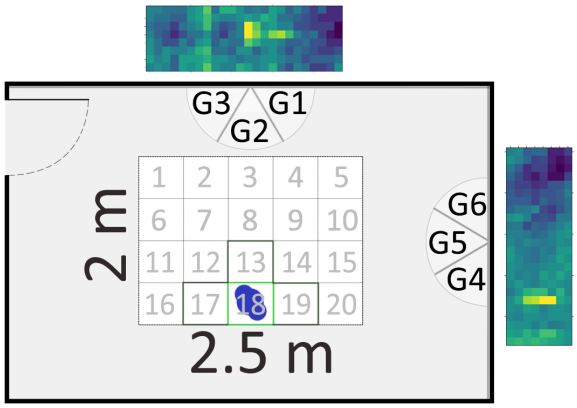

Figure 6: Visualization of the conducted setup for the experiment. One person (blue point) equipped with a Dell headset for position determination purposes moves within the predefined measurement area (2 × 2.5 m). The measurement area is divided into a 4 × 5 grid field. Both sensor clusters (G1-G3, G4-G6) capture the scene. Afterwards, the data is evaluated to deduce the true grid location of a person. Both the score for the actual grid position (light green) as well as the accuracy score for the neighborhood (dark green) will be evaluated.

3 RESULTS

The main objective of the measurement by the previously described system is the proof of concept for the IR sensor cluster localization method and the comparison of whether the use of such clusters has a beneficial effect on the accuracy of the localization. Table 1 shows the results of the measurement with 2128 samples for both tested evaluation criteria. 25 % of the data were used for testing, the remaining 75 % functioned as training data for classification. The multiclass classification of the SVM is done by a one-vs-all scheme where separate classifiers are learned for each different grid label ranging from 1 to 20 as seen in Figure 6.

In addition to the accuracy of the correct grid determination, Fig. 7 also shows an exemplary probability heat map at one point in time. With these two visualization methods it is easier to evaluate the results correctly.

Table 1: SVM classification accuracy results based on Eq. 4 for three cases where either the data of one sensor cluster is used or the data of both. Scores for on point classification (single grid field) and a neighborhood of four classification (neighborhood grid fields) are shown.

SVM Accuracy	G1-G3	G4-G6	G1-G6
Single	0.689	0.567	0.731
Neighborhood	0.812	0.789	0.930

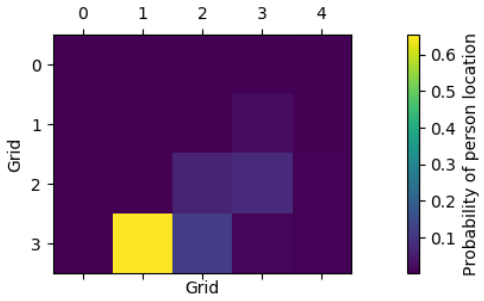

Figure 7: Exemplary visualization of a probability heat map for the predefined grid field. Based on the classification results, the location probabilities for a person are shown on each particular grid.

4 DISCUSSION

The results indicate that it is possible to perform indoor localization on the basis of low-resolution IR sensors. Table 1 shows the accuracy of the classification for detection in a single grid field and also for detection within a neighborhood of four. As assumed in advance, classification works best if the data of both clusters is used (93.0 % accuracy for neighborhood classification and 73.1 % for single classification). In the case where only one cluster measures data at a time, either an accuracy of 68.9 % (G1-G3) or 56.7 % (G4-G6) is achieved for the single grid classification or 81.2 % (G1-G3) or 78.9 % (G4-G6) for the neighborhood classification. The difference between the performance of G1-G3 and G4-G6 can be explained by the fact that G4-G6 is positioned on the wall where the measurement area is less broad and therefore collects less discriminative information. We assume that the accuracy of G1-G3 suffers from the greater depth of 2.5 m, since the depth only plays an indirect role via the number of pixels of a person to be detected.

Overall, the accuracy of the single grid field classification method is relatively poor even when both clusters (G1-G6) are integrated. The single grid evaluation criteria emphasizes exact localization decisions from very low-resolution data while also suffering from quantization error. Therefore, a low performance is expected. Depending on the location of the person, one is often in the transition area between two grids, so that a clear assignment becomes difficult. For this reason, the visualization of the heat map used in Fig. 7 is more suitable for assessment purposes. The advantage of this type of visualization is that if there are more grids with an increased probability of the person's localization, it becomes immediately apparent that the person is presumably in the transition area of the grids. Thus, a heatmap is better suited to estimate the location of the person. In addition, the size of the subdivided grid fields most probably is an influencing factor that has an important impact on the accuracy of the classifier. This particular aspect could be examined in future work.

5 CONCLUSIONS

In this paper, we developed a cost-efficient indoor localization setup based on the combination of multiple low-resolution IR array sensors which is independent of ambient lighting. By using the temperature data output of each 8×24 pixel sensor cluster it was possible to locate a person in a predefined area of 2.5×2 m, which was further sliced into 20 distinguishable 50×50 cm grids. It was then possible to deduce the person's location by applying a SVM classification.

Since this work represents an early feasibility study, further points will have to be addressed in future research work. It is planned to compare further machine learning methods for the classification accuracy. Moreover, it is conceivable to increase the number of persons to be localized simultaneously, to enlarge the measuring area, to replace the subdivision into individual grids by an exact estimation of the x- and y-coordinates, to detect several states such as "sitting", "falling" and "lying" by taking the height into account, to perform a comprehensive investigation of different classification techniques and to carry out the entire setup in a realistic environment with additional sources of interference such as heating or solar radiation.

ACKNOWLEDGEMENTS

This work was funded by the German Ministry for Education and Research (BMBF) within the research project Nursing Care Innovation Center (grant 16SV7819K).

REFERENCES

Adafruit (2017). Adafruit circuitpython amg88xx. https://github.com/adafruit/Adafruit_CircuitPython_AMG88xx.

Basu, C. and Rowe, A. (2015). Tracking motion and proxemics using thermal-sensor array. *arXiv preprint arXiv:1511.08166*.

Beltran, A., Erickson, V. L., and Cerpa, A. E. (2013). Thermosense: Occupancy thermal based sensing for hvac control. In *Proceedings of the 5th ACM Workshop on Embedded Systems For Energy-Efficient Buildings*, pages 1–8. ACM.

Fan, X., Zhang, H., Leung, C., and Shen, Z. (2017). Robust unobtrusive fall detection using infrared array sensors. In *Multisensor Fusion and Integration for Intelligent Systems (MFI), 2017 IEEE International Conference on*, pages 194–199. IEEE.

Gerka, A., Pfingsthorn, M., Lupkes, C., Sparenberg, K., Frenken, M., Lins, C., and Hein, A. (2018). Detecting the number of persons in the bed area to enhance the safety of artificially ventilated persons. In *2018 IEEE 20th International Conference on e-Health Networking, Applications and Services (Healthcom)*, pages 1–6. IEEE.

Gonzalez, L. I. L., Troost, M., and Amft, O. (2013). Using a thermopile matrix sensor to recognize energy-related activities in offices. *Procedia Computer Science*, 19:678–685.

Hsu, C.-W., Chang, C.-C., Lin, C.-J., et al. (2003). A practical guide to support vector classification.

Jeong, Y., Yoon, K., and Joung, K. (2014). Probabilistic method to determine human subjects for low-resolution thermal imaging sensor. In *Sensors Applications Symposium (SAS), 2014 IEEE*, pages 97–102. IEEE.

Mashiyama, S., Hong, J., and Ohtsuki, T. (2015). Activity recognition using low resolution infrared array sensor. In *Communications (ICC), 2015 IEEE International Conference on*, pages 495–500. IEEE.

Mubashir, M., Shao, L., and Seed, L. (2013). A survey on fall detection: Principles and approaches. *Neurocomputing*, 100:144–152.

Niehorster, D. C., Li, L., and Lappe, M. (2017). The accuracy and precision of position and orientation tracking in the htc vive virtual reality system for scientific research. *i-Perception*, 8(3):2041669517708205.

Panasonic (2016). White paper: Grid-eye state of the art thermal imaging solution. Accessed: 2018-11-16.

Panasonic (2017). Data sheet: Infrared array sensor grid-eye (amg88). Accessed: 2018-11-18.

Pedregosa, F., Varoquaux, G., Gramfort, A., Michel, V., Thirion, B., Grisel, O., Blondel, M., Prettenhofer, P., Weiss, R., Dubourg, V., Vanderplas, J., Passos, A., Cournapeau, D., Brucher, M., Perrot, M., and Duchesnay, E. (2011). Scikit-learn: Machine learning in Python. *Journal of Machine Learning Research*, 12:2825–2830.

Rapoport, M. (2012). The home under surveillance: A tripartite assemblage. *Surveillance & Society*, 10(3/4):320.

Razavi, S. S., Fathi, M., and Hajiesmaeili, M. (2016). Intensive care at home: An opportunity or threat. *Anesthesiology and pain medicine*, 6(2).

Shetty, A. D., Shubha, B., Suryanarayana, K., et al. (2017). Detection and tracking of a human using the infrared thermopile array sensorgrid-eye. In *Intelligent Computing, Instrumentation and Control Technologies (ICICICT), 2017 International Conference on*, pages 1490–1495. IEEE.

Trofimova, A. A., Masciadri, A., Veronese, F., and Salice, F. (2017). Indoor human detection based on thermal array sensor data and adaptive background estimation. *Journal of Computer and Communications*, 5(04):16.

World Health Organization (2015). *World report on ageing and health*. World Health Organization.